The Abdus Salam International Centre for Theoretical Physics

United Nations Educational, Scientific and Cultural Organization

IAEA International Atomic Energy Agency

1953-10

International Workshop on the Frontiers of Modern Plasma Physics

14 - 25 July 2008

Laboratory Reproduction of Auroral Magnetospheric Radio Wave Sources.

K. Ronald

University of Strathclyde
Division of Plasmas
U.K.

Strada Costiera 11, 34014 Trieste, Italy - Tel. +39 040 2240 111; Fax +39 040 224 163 - sci_info@ictp.it, www.ictp.it

Laboratory Reproduction of Auroral Magnetospheric Radio Wave Sources

K. Ronald*,
D.C. Speirs*, S.L. McConville*, K.M. Gillespie*, A.D.R. Phelps*,
A.W. Cross*, R. Bingham*+, C.W. Robertson*, C.G. Whyte*, I. Vorgul#,
R.A. Cairns#, B.J. Kellett+, and W. He*

** SUPA and Department of Physics, University of Strathclyde, Glasgow, G4 0NG, UK.*
 # School of Mathematics and Statistics, University of St Andrews, St Andrews, Fife, KY16 9SS, UK.
+ STFC Rutherford Appleton Laboratory, Chilton, Didcot, Oxfordshire OX11 0QX, UK.

Introduction - The Auroral Kilometric Radiation

- Intense RF emission at high altitudes (~1.5 – 3 Earth radii) within a large region of plasma depletion (the auroral density cavity), at frequencies of ~300kHz
- Discrete components of emission typically ~1kHz in bandwidth
- Within the source region the emissions have been observed to be polarised in the extraordinary (X) mode
- At certain altitudes, frequency components of emission are observed to extend down to the local relativistic electron cyclotron frequency Ω_{ce}/γ
- These emissions are observed in conjunction with the formation of a horseshoe distribution function in electron velocity space
- Total RF output power ranges between 10^7 – 10^9 Watts. Efficiency of emission is ~1-2% [Gurnett1974]

Cyclotron Resonant Instability

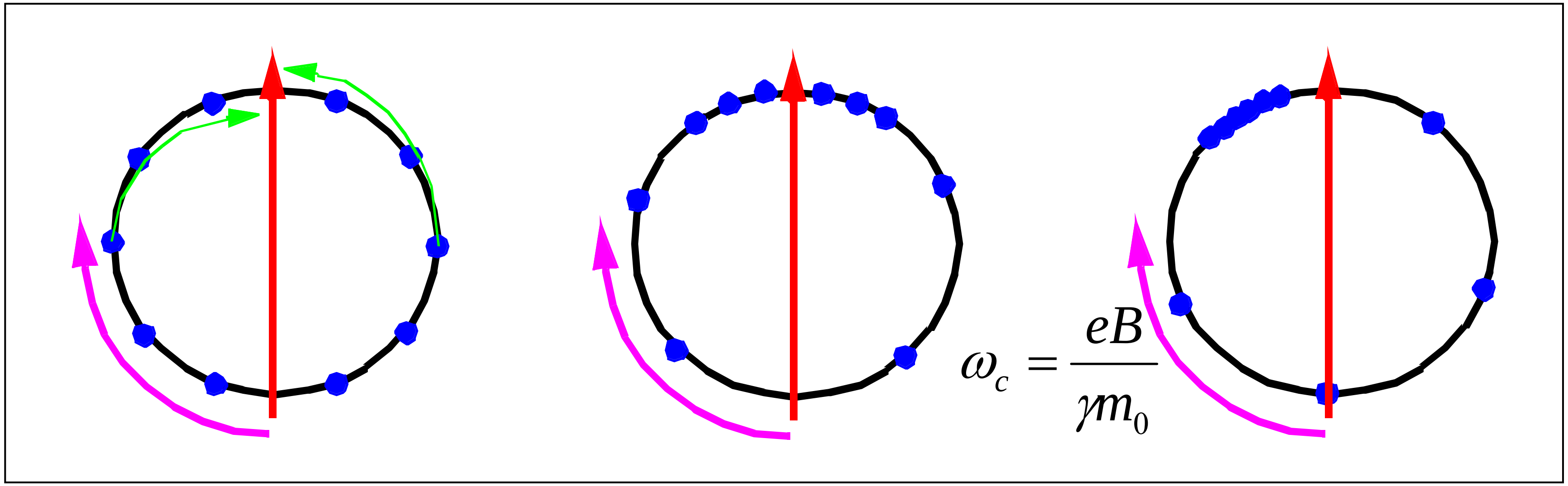

- Electrons gyrate in close synchronism with a rotating electric field vector
- Bunching occurs due to modulation of the electron energy via the relativistic cyclotron frequency- this is fundamentally a relativistic phenomenon
- If the cyclotron frequency is slightly less than the wave frequency then net energy extraction may occur
- Saturation arises when phase trapping occurs

Horseshoe distribution formation

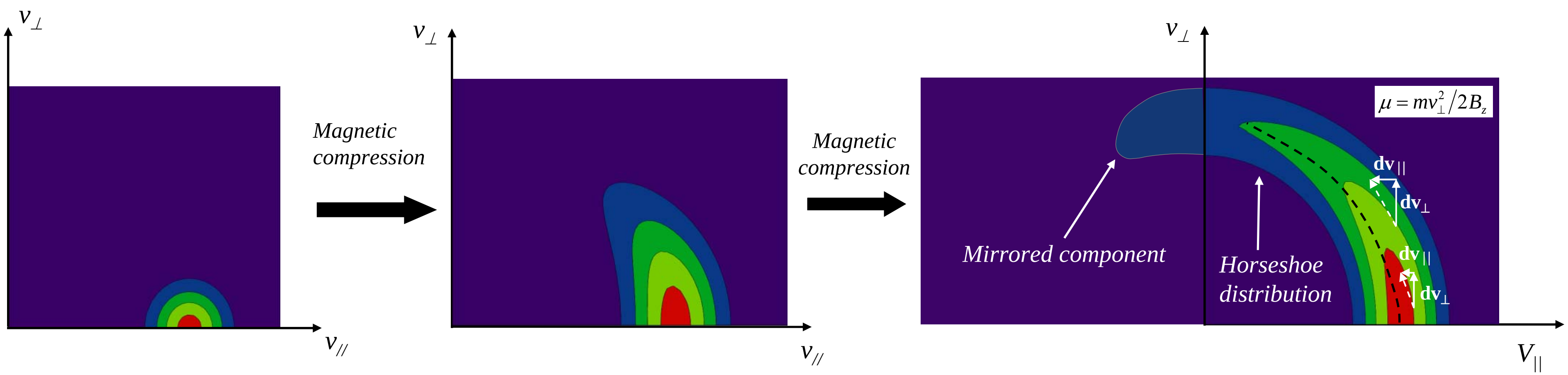

- When an electron propagates into an increasing axial magnetic field a horseshoe distribution may arise

- Reason - conservation of the magnetic moment, μ

$$\mu = \frac{mv_\perp^2}{2B_0}$$

- Conversion of axial velocity $v_{//}$ into perpendicular velocity $v_\perp$, results in an increase in electron pitch factor, α.

$$\alpha = v_\perp / v_{//}$$

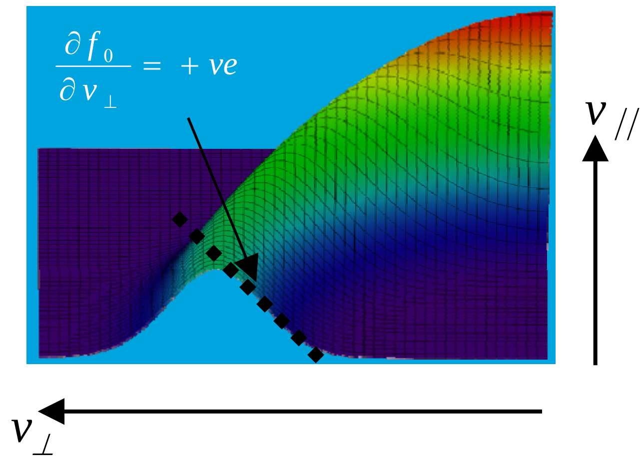

Space : Laboratory

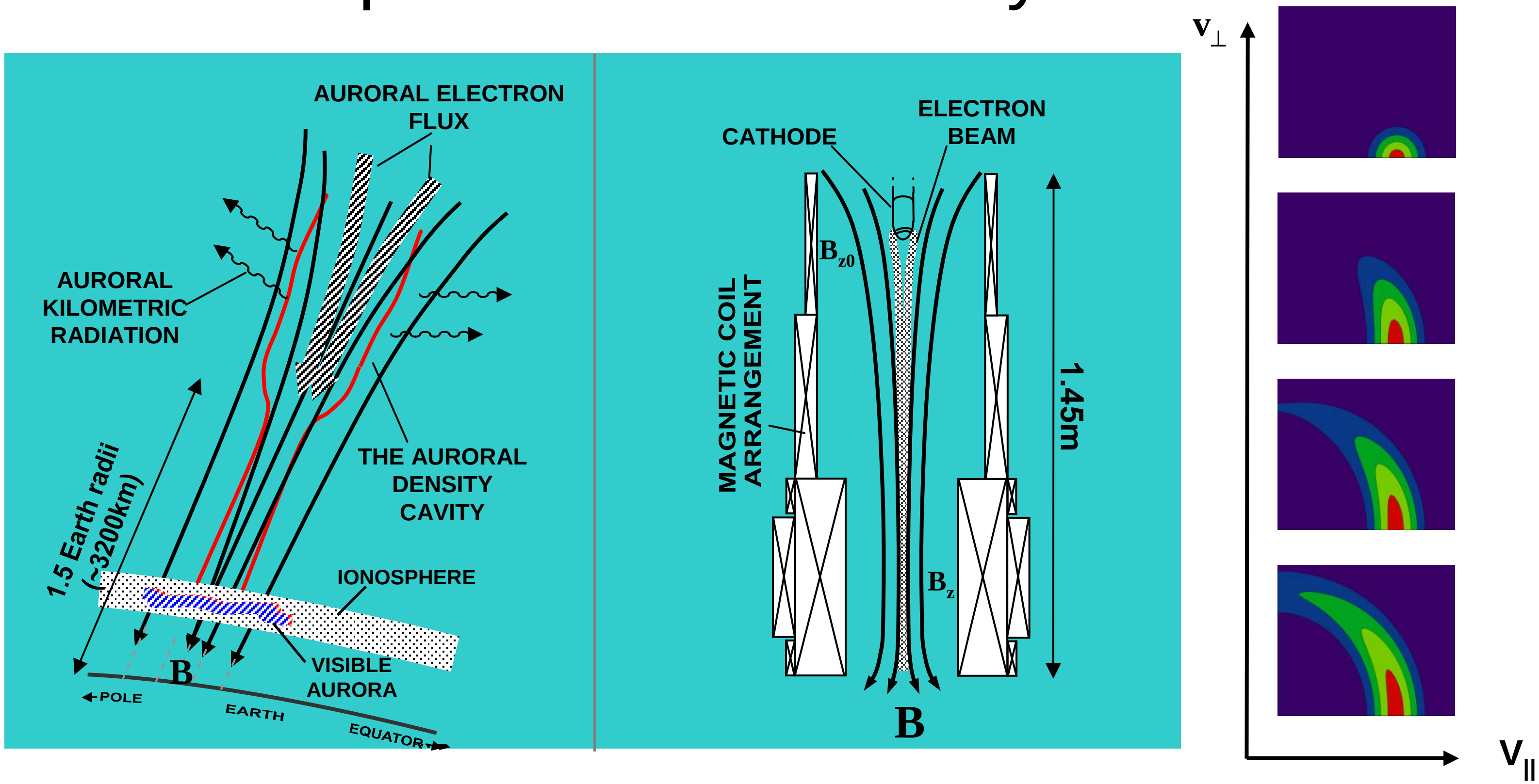

<u>Objectives</u>

- To form in the laboratory an electron beam with velocity distribution comparable to the magnetosphere
- Scale radiation resonance to the microwave range
- Characterise the electron beam parameters and take microwave measurements as function of magnetic compression
- Compare with numerical simulation and magnetospheric results

Similar astrophysical radio sources
CU Virginis

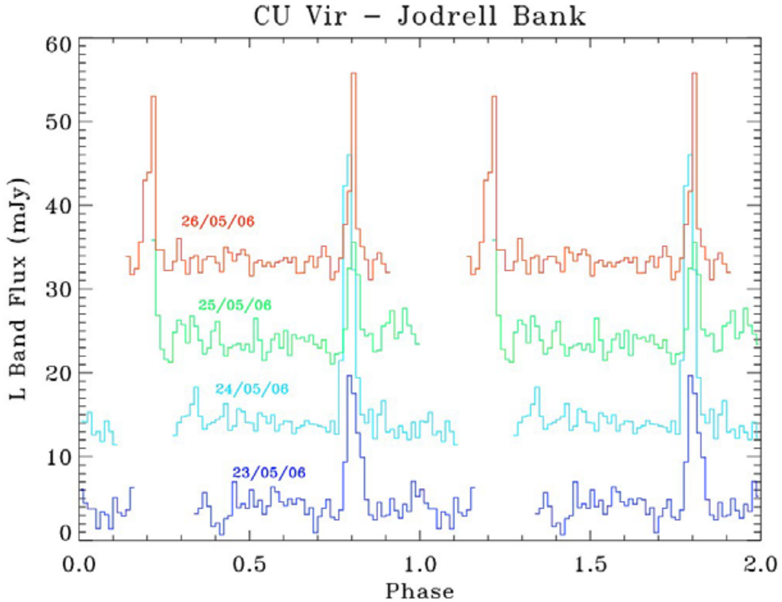

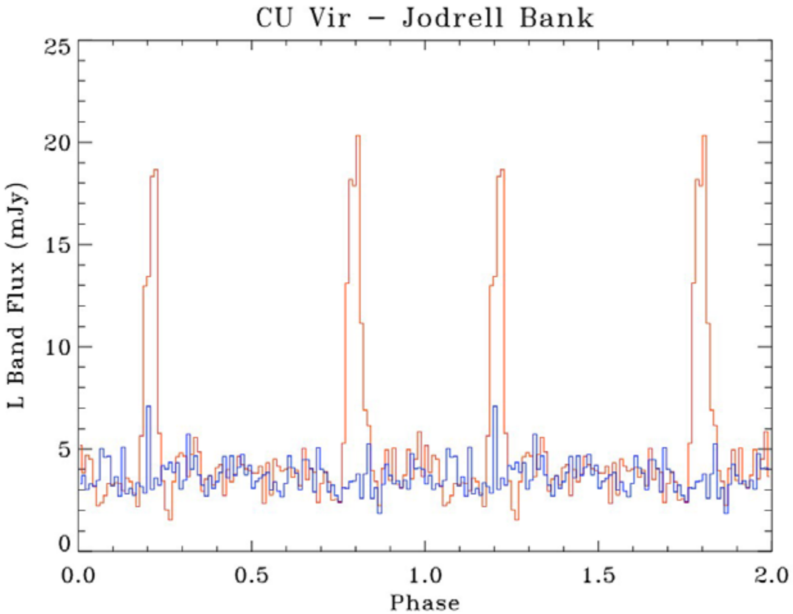

- Recently observed by the telescopes at Jodrell Bank
- Highly reproducible L Band microwave emission from polar regions
- Strongly circularly polarised

Polarisation and dispersion

- Natural emission is in the X-mode, AC E-field and wavevector normal to static B-field
- Perpendicular wavevector can be achieved by waveguide modes near cut-off

$$\omega = \omega_{ce} + k_{\|} v_{\|}$$

$$\omega_{ce} = 2\pi f_c = \frac{eB_z}{\gamma m_0}$$

$$\gamma = 1 + \frac{eV}{m_o c^2} = \left[1 - \frac{v^2}{c^2}\right]^{-\frac{1}{2}}$$

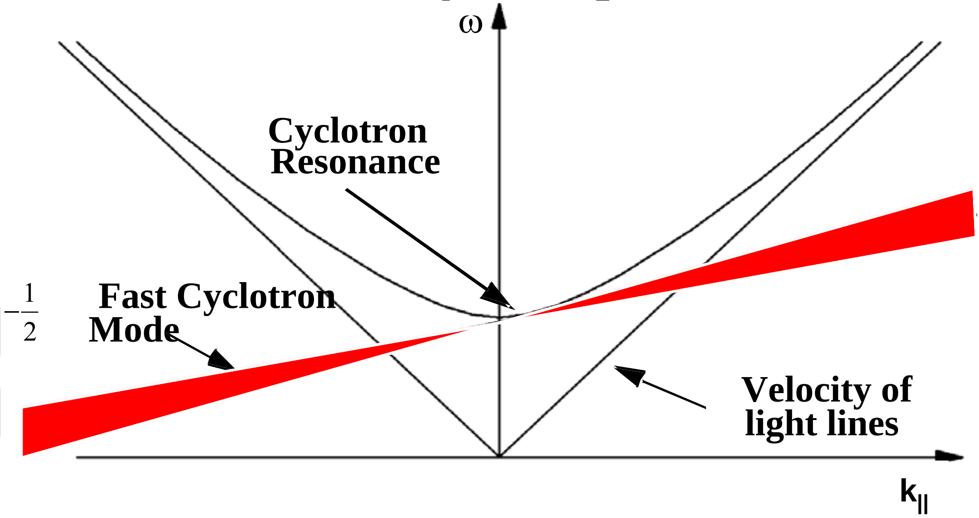

Transverse field components for modes of cylindrical waveguides

- Near cut-off modes are required to give the correct propagation orientation and minimise the Doppler broadening
- TE modes have finite transverse electric field when $k_{\|} \rightarrow 0$
- TM modes have zero transverse electric field when $k_{\|} \rightarrow 0$
- Using TE modes near cut-off gives an approximation to the X-mode

Experimental schematic

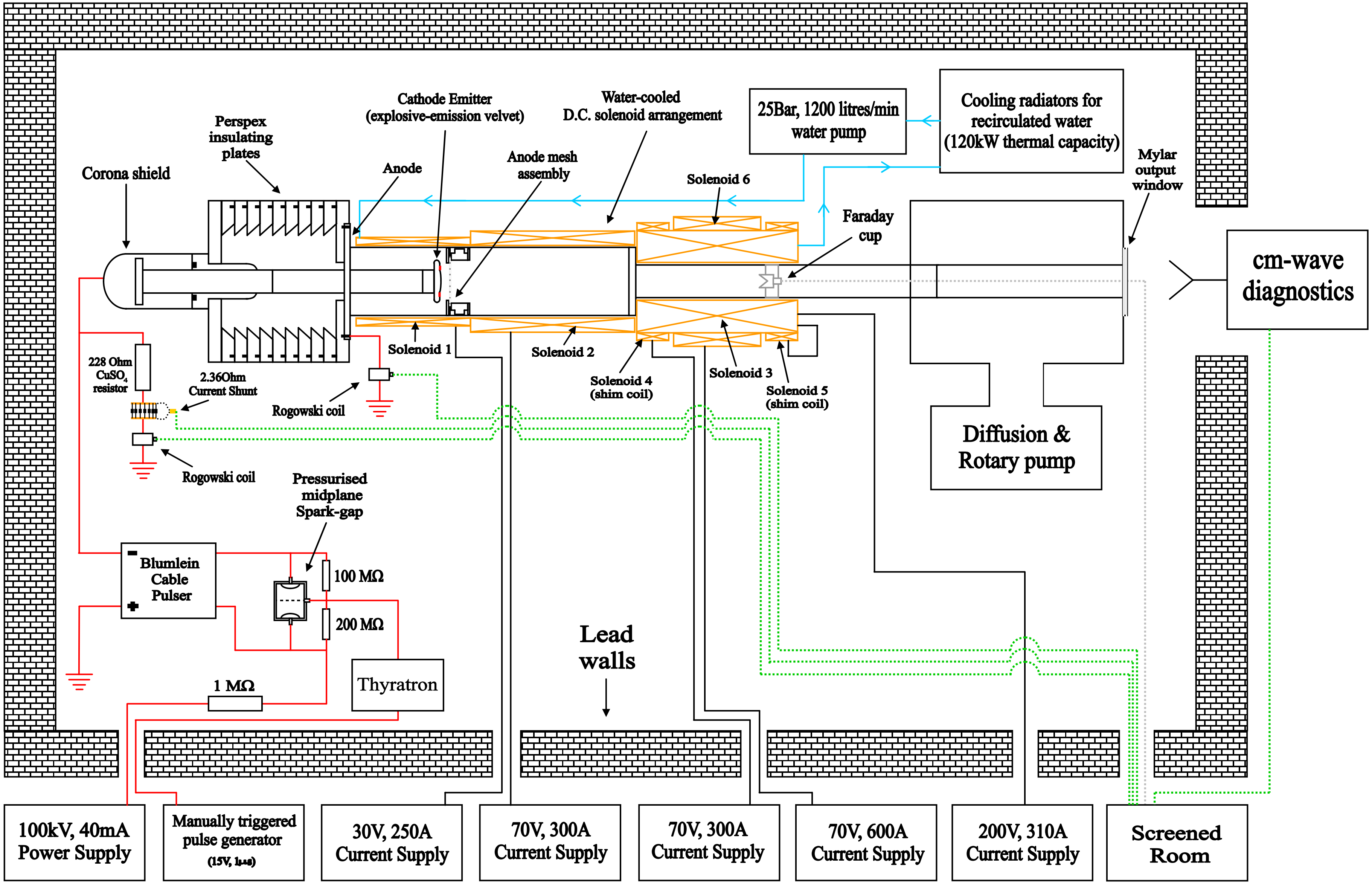

Solenoid configuration

- Insulated OFHC copper tubing, 7mm OD, 2mm ID (total length >1km) wound on non-magnetic formers, tubing is core cooled by water at 20Bar
- Drive 5 solenoids independently up to 300A with 120kW DC power supplies
- Flexible control of the magnetic field configuration

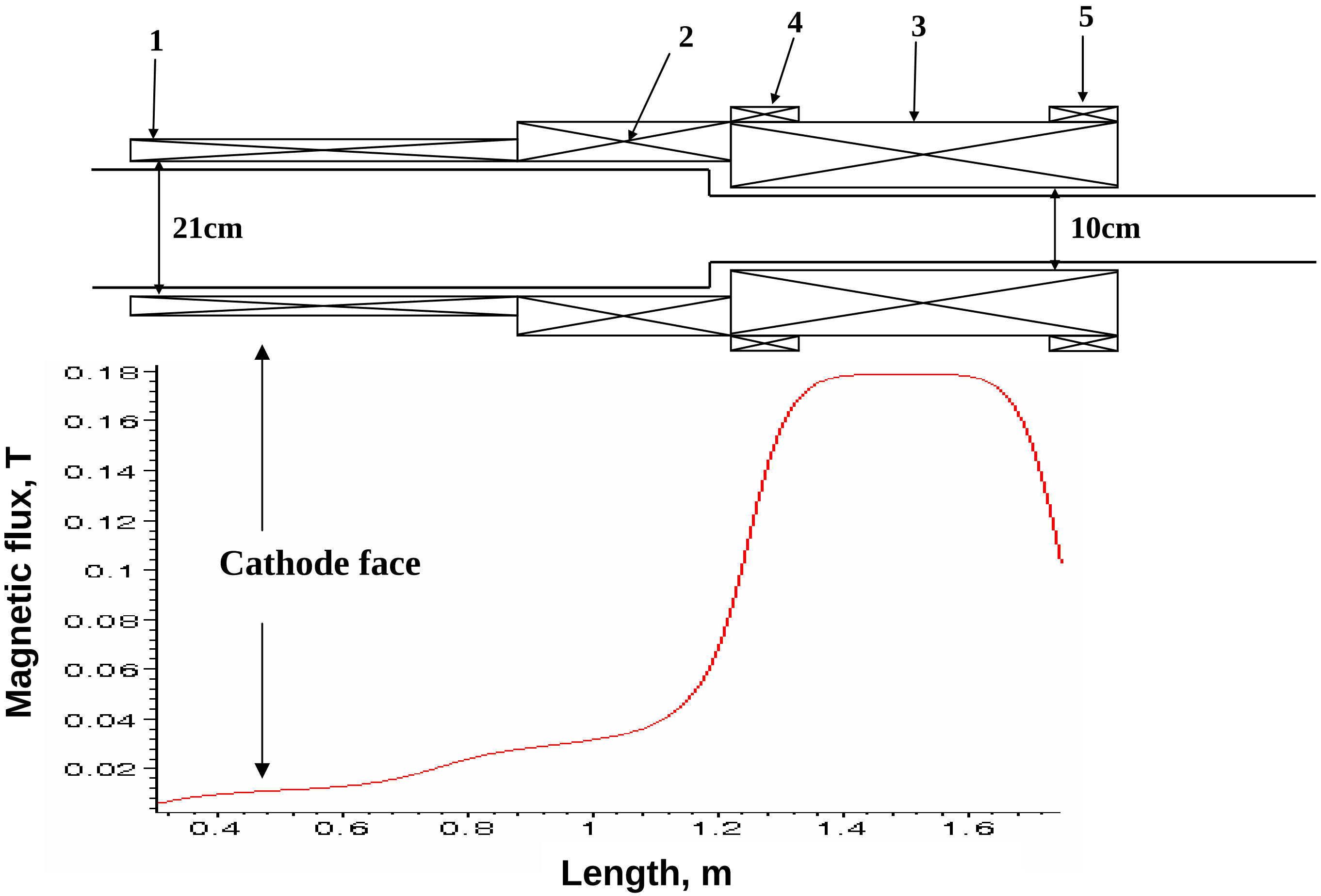

Experimental apparatus

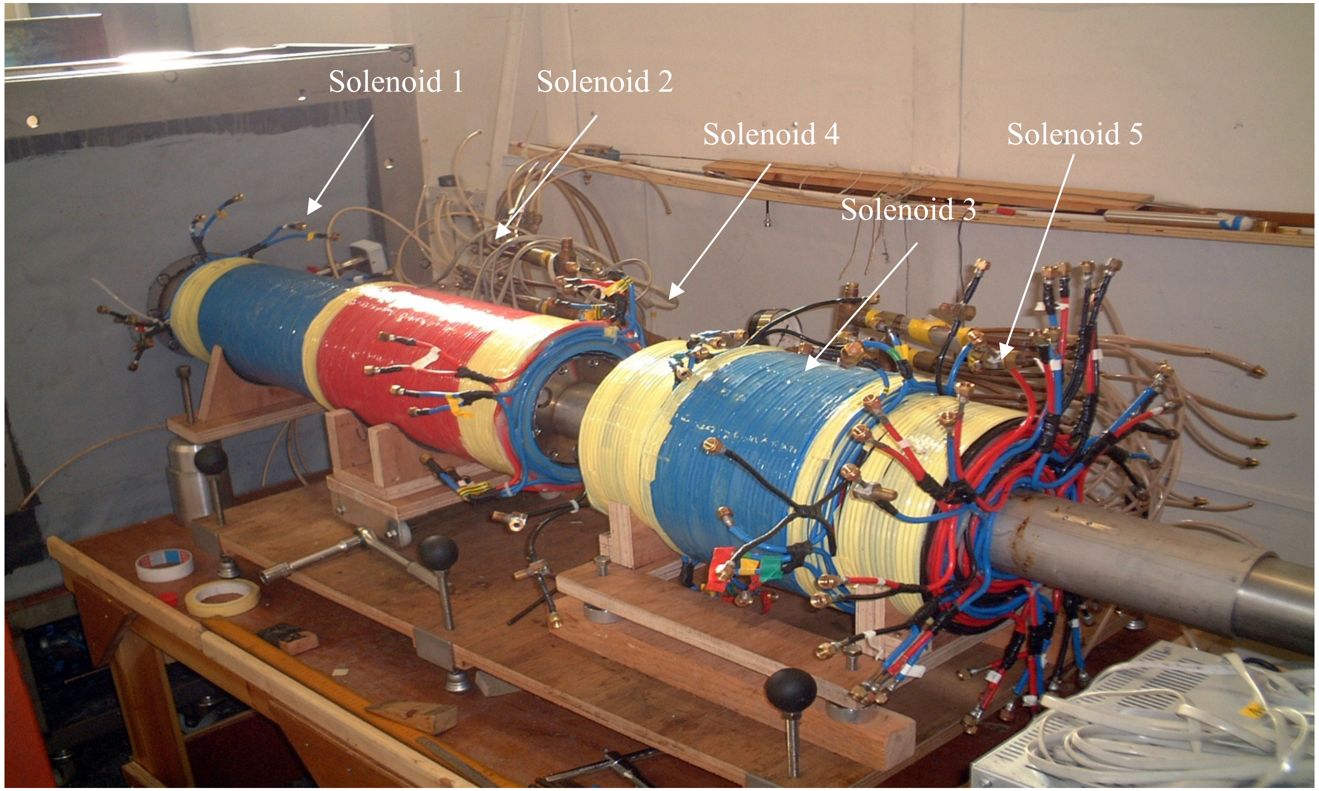

Solenoid 1: 4 Layers, Length = 0.5m, R_i = 0.105m, Current = 75A.

Solenoid 2: 2 Layers, Length = 0.45m, R_i = 0.105m, Current = 60A.

Solenoid 3: 10 Layers, Length = 0.5m, R_i = 0.05m, Current = 250A.

Solenoid 4: 2 Layers, Length = 0.11m, R_i = 0.12m, Current = 250A.

Solenoid 5: 2 Layers, Length = 0.11m, R_i = 0.12m, Current = 250A.

Vacuum spark electron injector

- Velvet electron emitter secured to a planar metallic surface facing a sparse mesh
- Cathode energised by a double Blumlein pulser generating over 75kV
- Field emission from velvet fibres combined with dielectric avalanche and surface flashover leads to a cathode plasma flare
- Space charge limited emission into vacuum gap
- Mesh concentrates electric field close to cathode

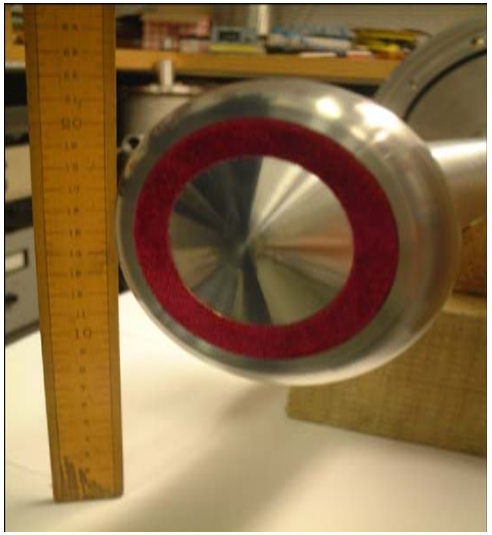

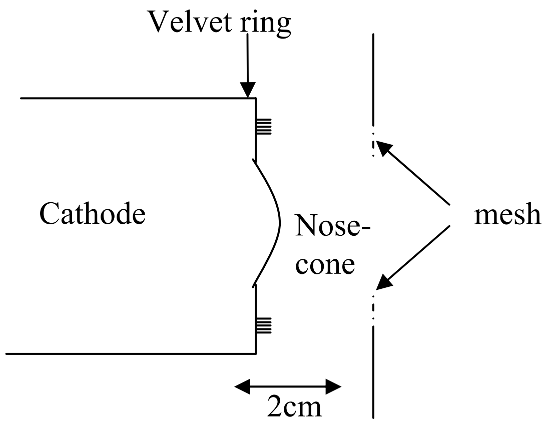

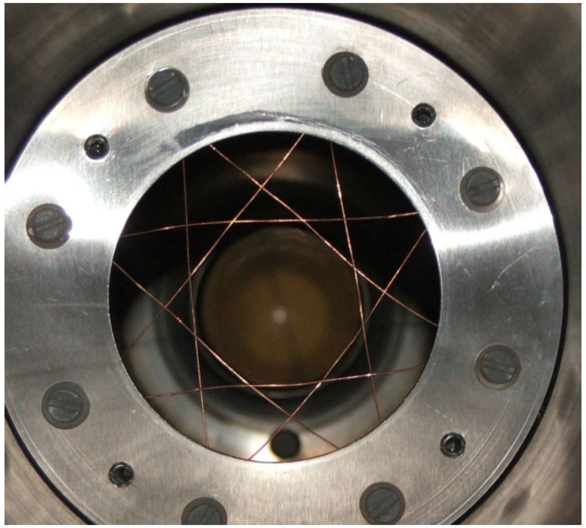

Experimental geometry

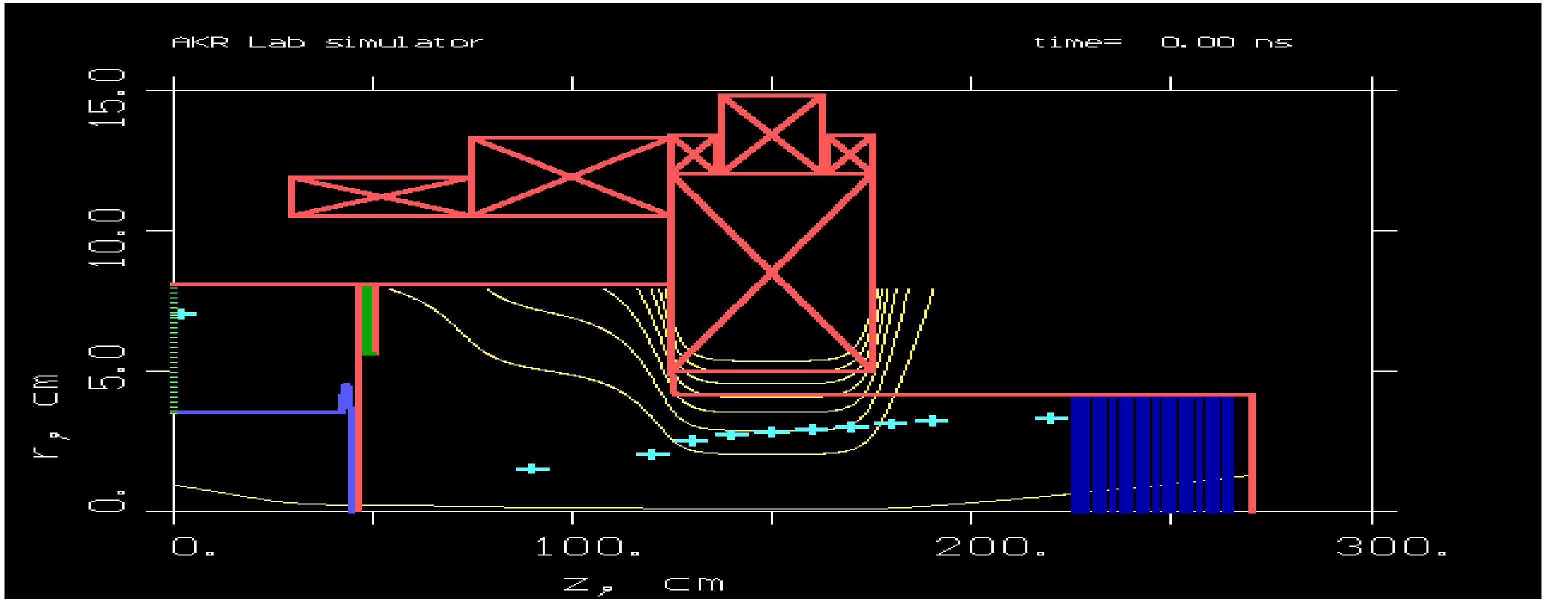

- Solenoid sizes set by power and cooling constraints
  - Sets dimensions of the rest of the apparatus
  - Electron gun region 16cm in diameter
  - Resonant region 8cm diameter and 20cm length
- Maximum possible fill factor ~50% (radius)
- Evacuated to <10^{-6}mBar

Electrical diagnostics

- Diode voltage:
  - Matching resistor (230Ω) in shunt with accelerator
  - Current measured by a Rogowski belt
- Diode current:
  - Rogowski belt (in ground connection of anode)
- Beam current:
  - Faraday cup feeding 50Ω shunt resistor

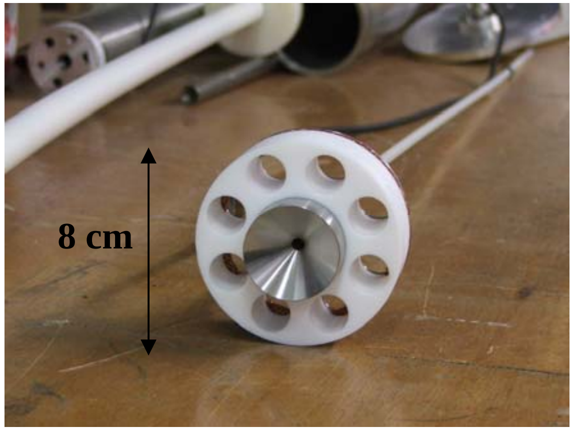

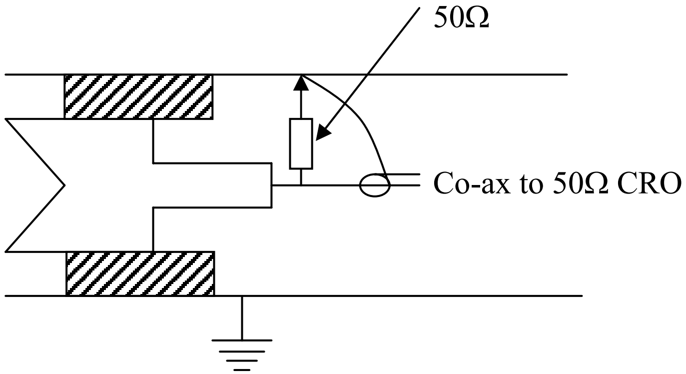

- Cup shaped to inhibit secondary escape

Microwave detection: Amplitude and Spectrum

- Waveguide 12 (single mode at 4.42GHz) or Waveguide 18 (single mode at 11.7GHz) antenna in far field of experiment output
- Fitted with calibrated attenuators
- Signals delivered to calibrated rectifying diodes
- Rectified signals measured on a 1.5GHz digital oscilloscope
- Spectrum measured by FFT of AC waveform captured by 12GHz DSO

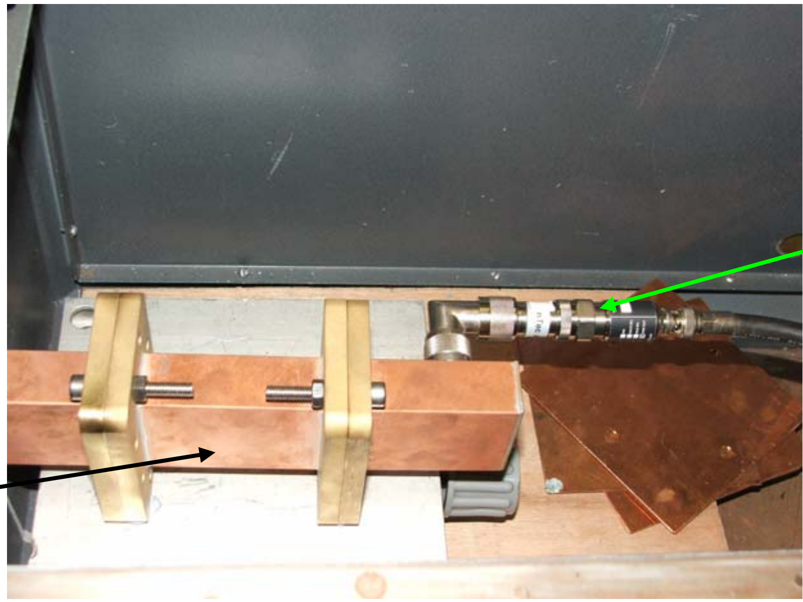

Microwave detection: Polarisation and Propagation

- Waveguide stub receiving antenna - output pattern and polarisation
- Waveguide attenuators and rectifying diodes - operating efficiency

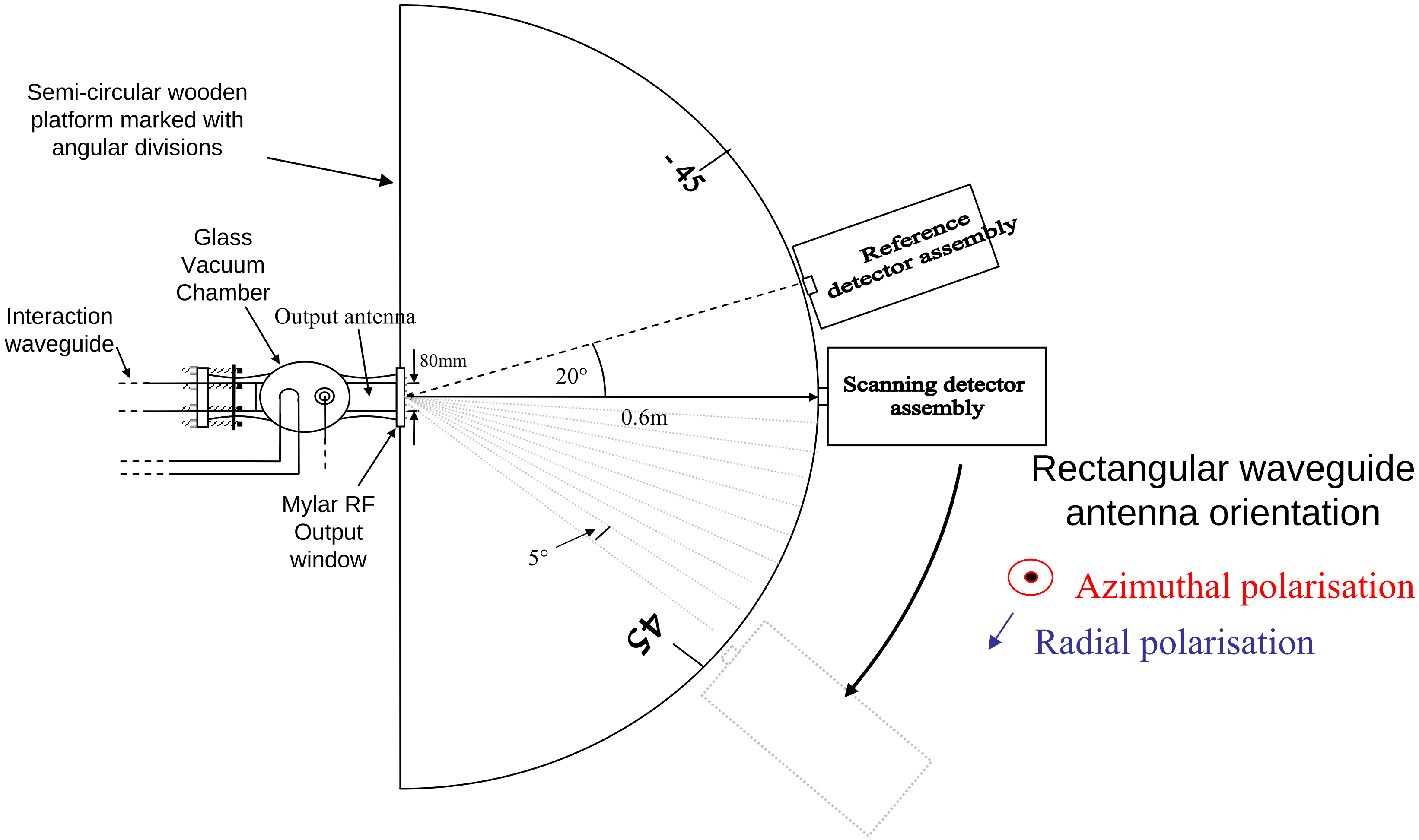

Experimental and numerical studies

- Beam formation investigated, numerically and experimentally
- Two regimes of radiation generation were studied:
  - 4.42GHz resonance, plateau B=0.18T
    - -Expected mode $TE_{0,1}$
    - -Relatively low order mode and magnetic flux density
    - -Potential to measure the electron velocity distribution
  - 11.7GHz resonance, plateau B=0.48T
    - -Resonant mode $TE_{0,3}$
    - -Highly overmoded, λ<<D, high magnetic flux density
    - -Chosen as most representative of magnetosphere

Experimental results: Beam formation

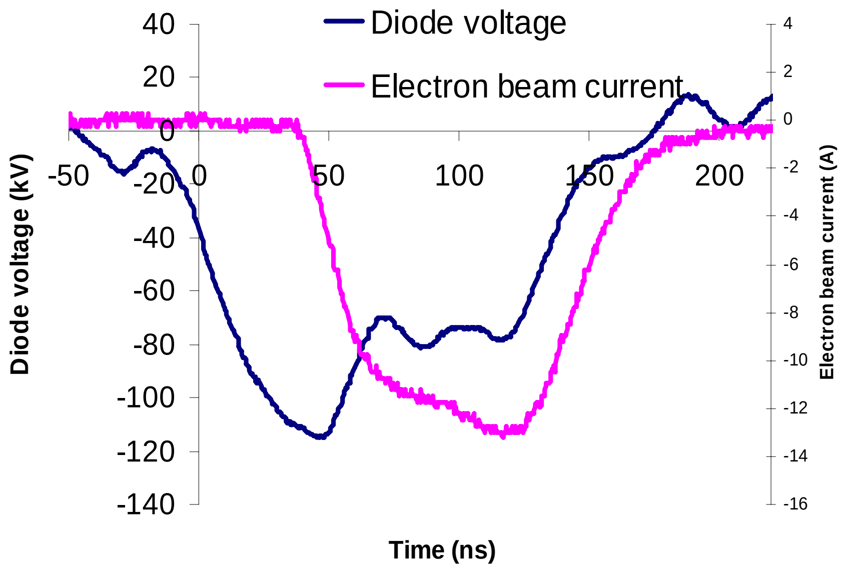

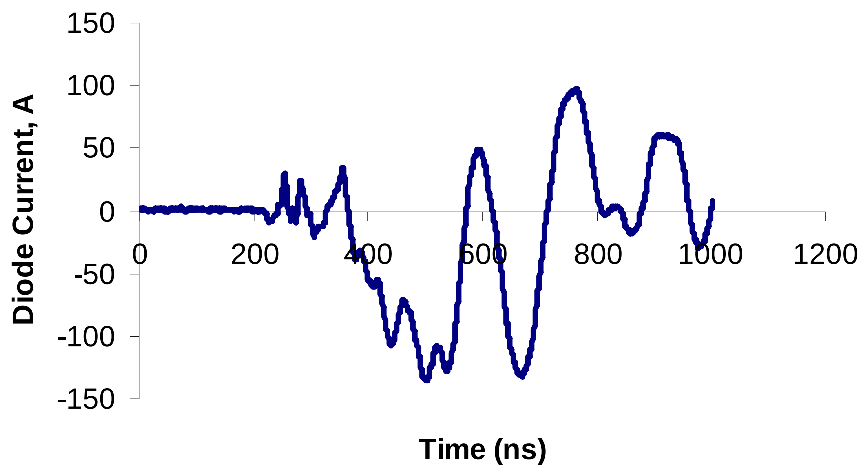

0.18T on main coil, beam voltage 75kV:

- Mirror Ratio of 17 gave I_{beam} of 12A
- Mirror Ratio of 9 gave I_{beam} of 34A
- Mirror Ratio of 4 gave I_{beam} of 44A

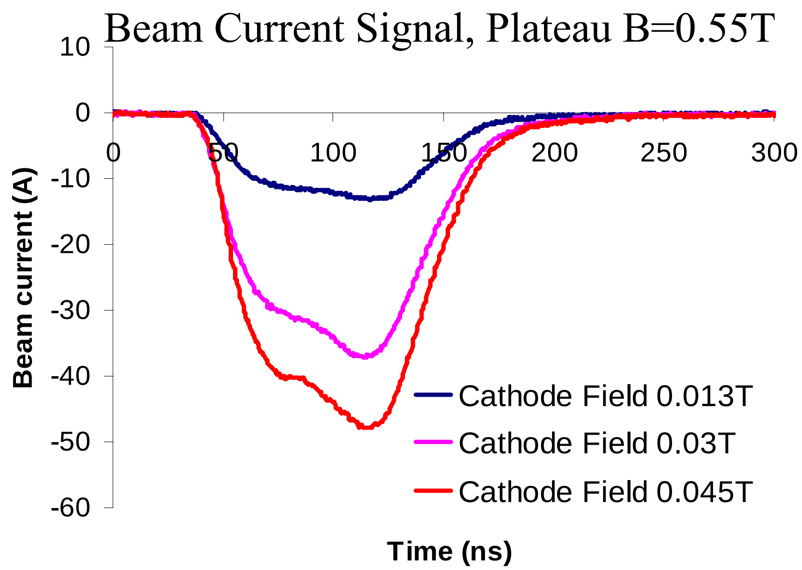

Beam transport measurements

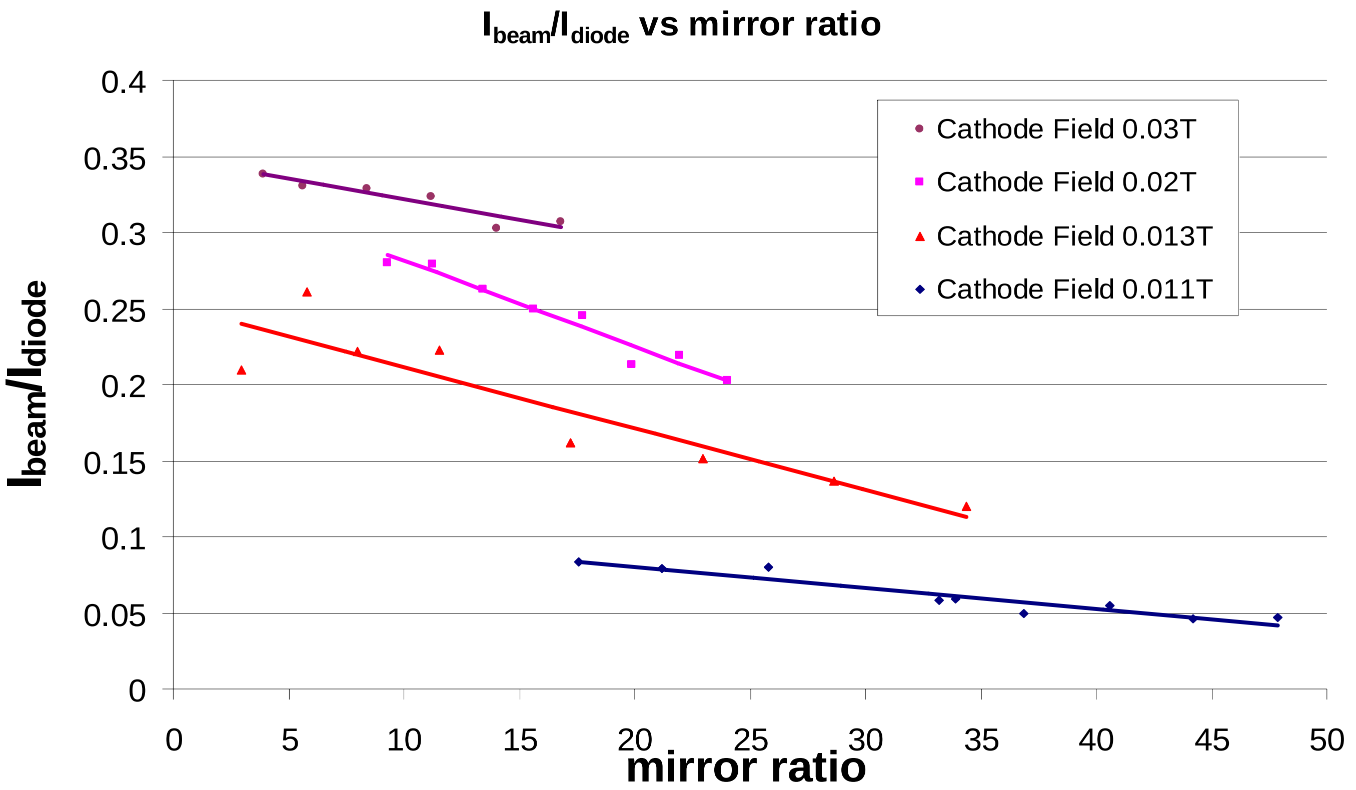

- Progressive decrease in current with increasing mirror ratio

  -Demonstrates formation of horseshoe distribution

Estimation of 1D number density

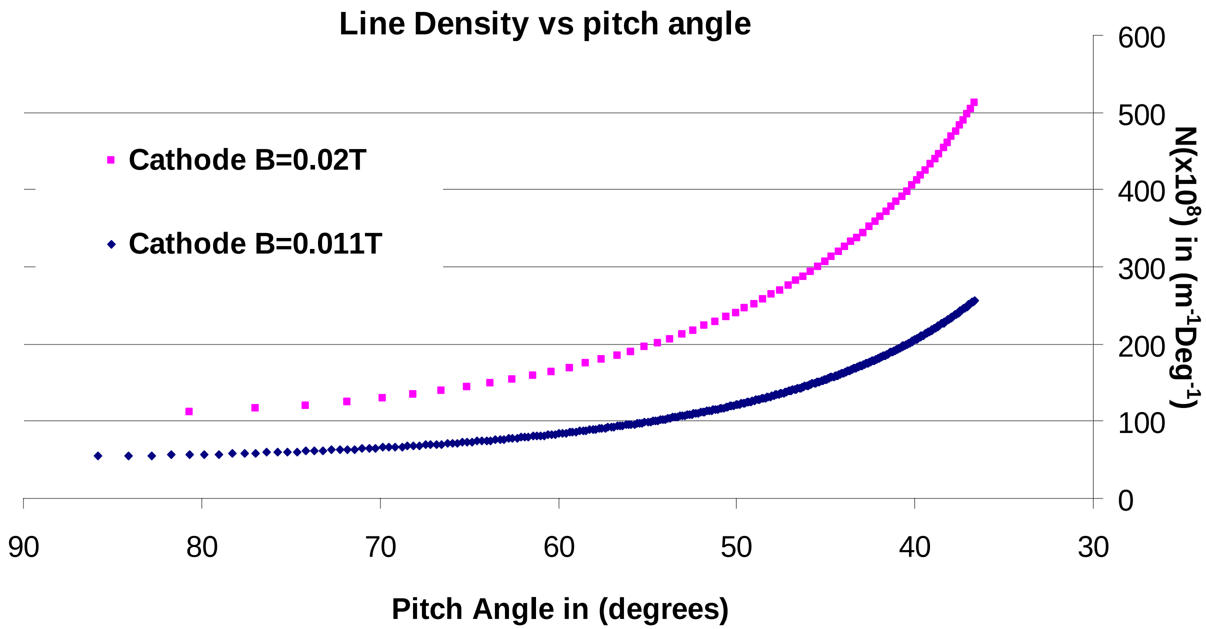

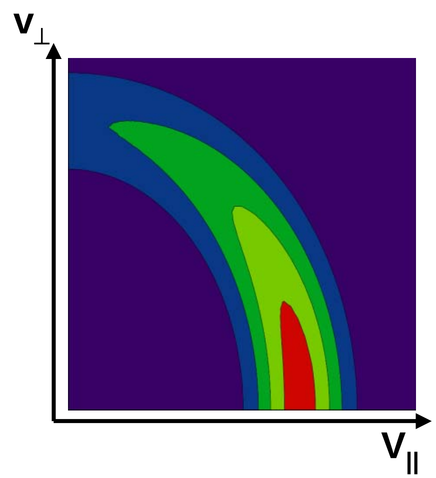

- Pitch angle is arctan($v_{\perp}$/ v_z)

4.42GHz Numerical simulations

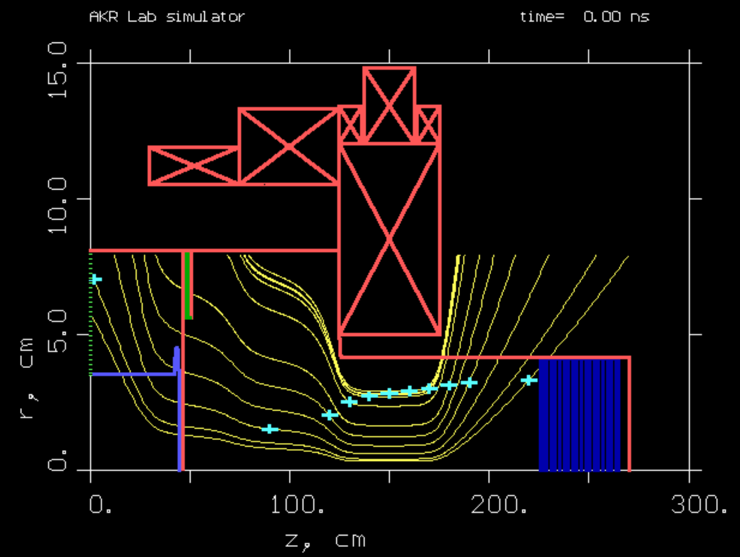

- Geometry programmed into KARAT, a 2D axi-symmetric PiC (Particle in Cell) code
- Highest η at 1% cyclotron detuning
  - Cathode B=0.011T, power ~20 kW, η=1.7%
  - Cathode B=0.02T, power ~50kW, η=2%

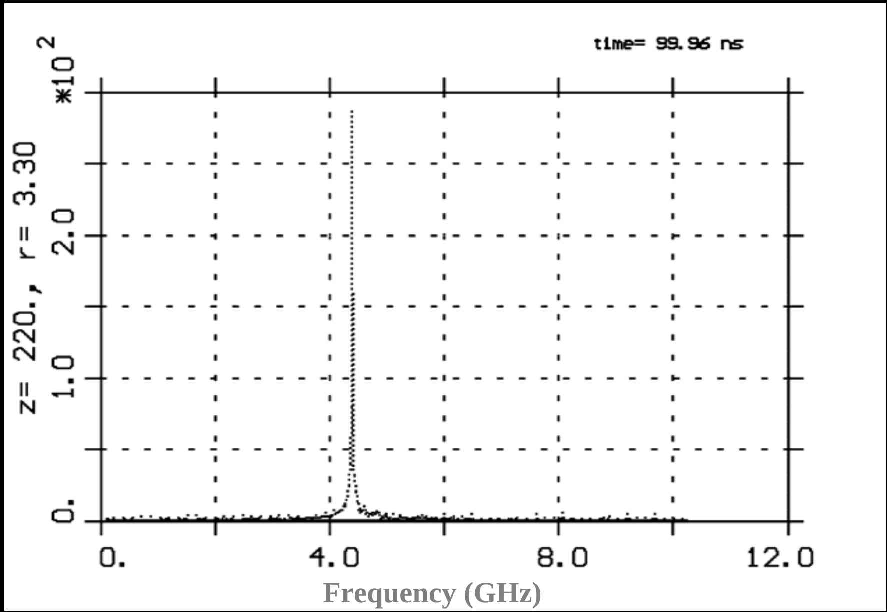

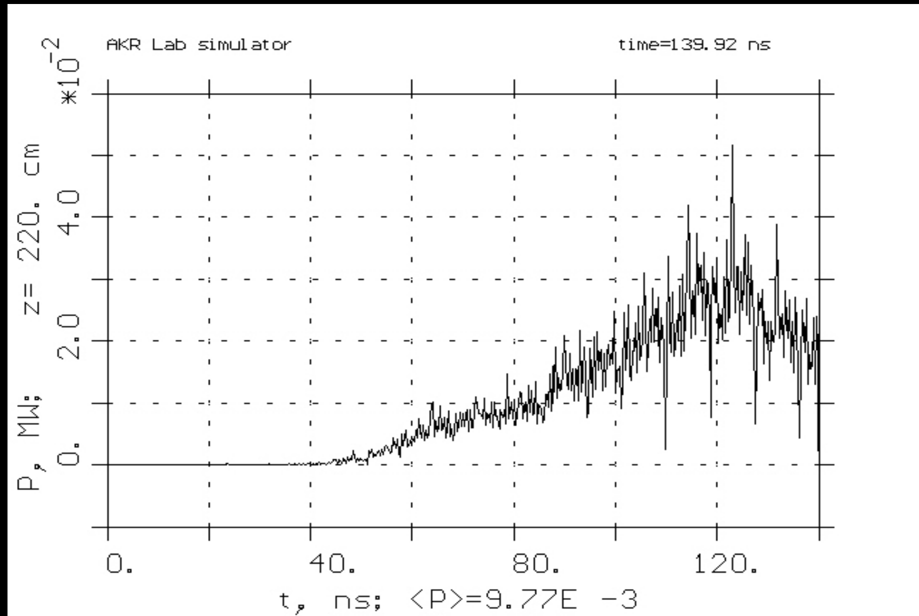

2D Simulations: Electron velocity distributions

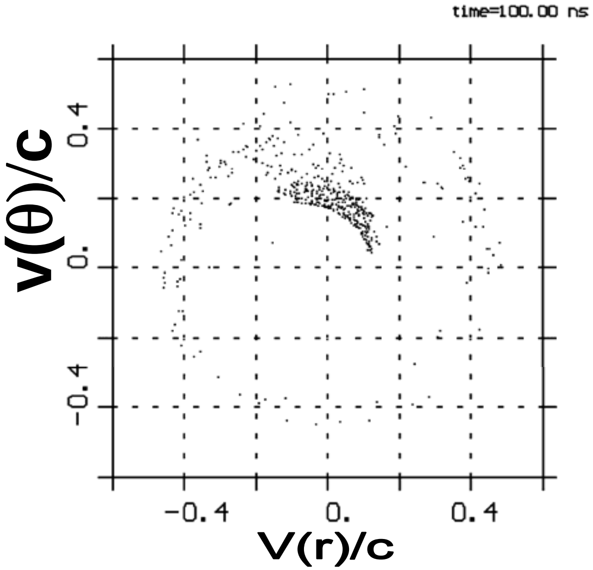

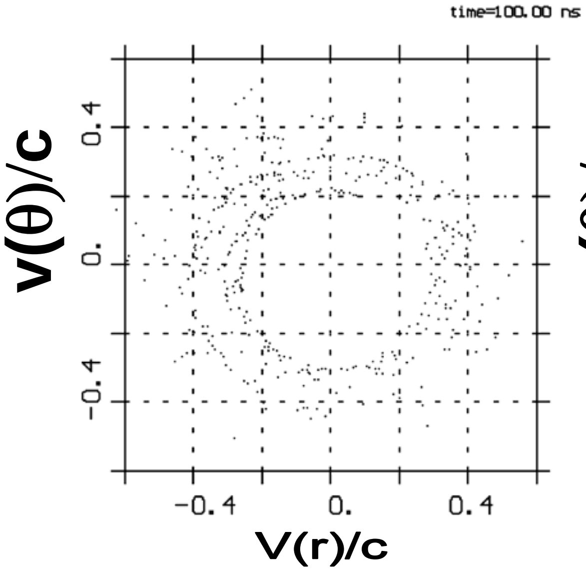

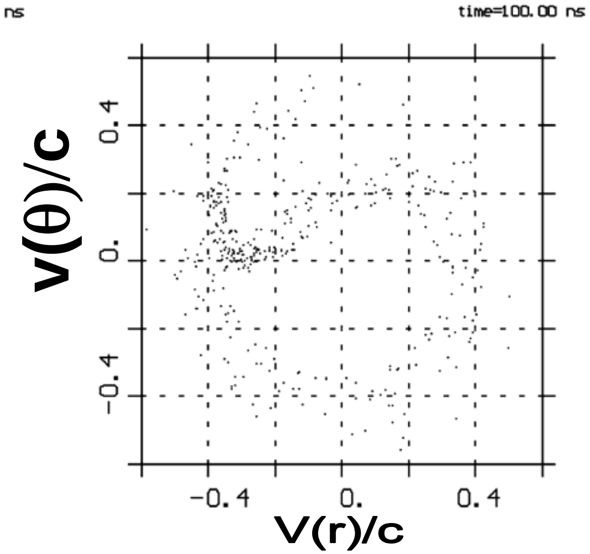

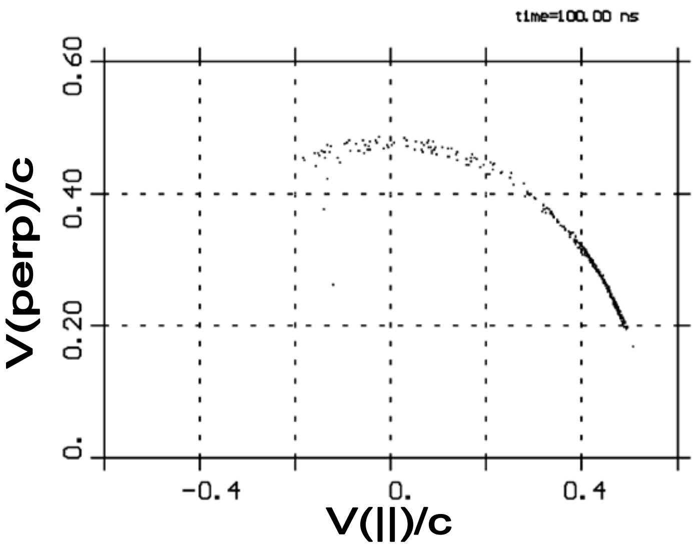

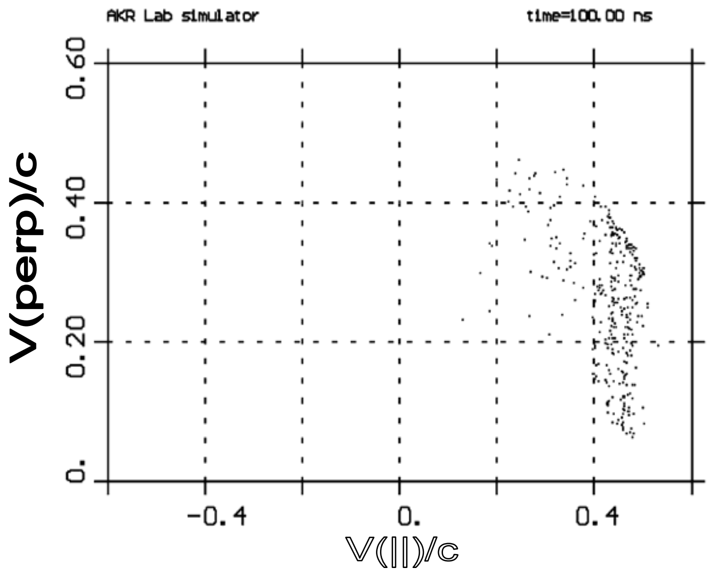

4.42GHz 3D Simulations

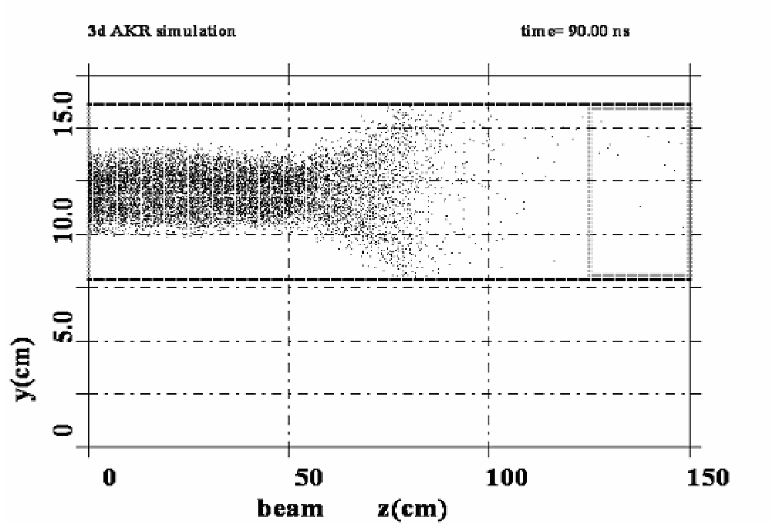

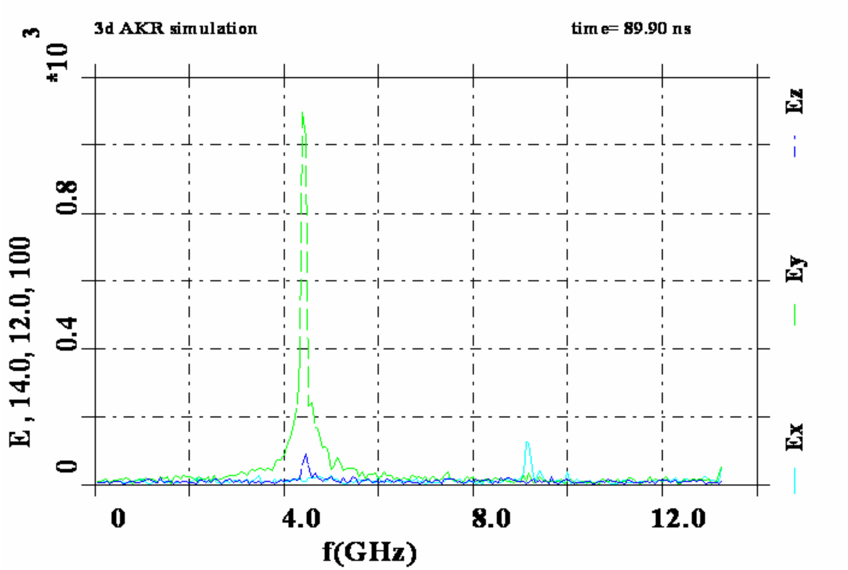

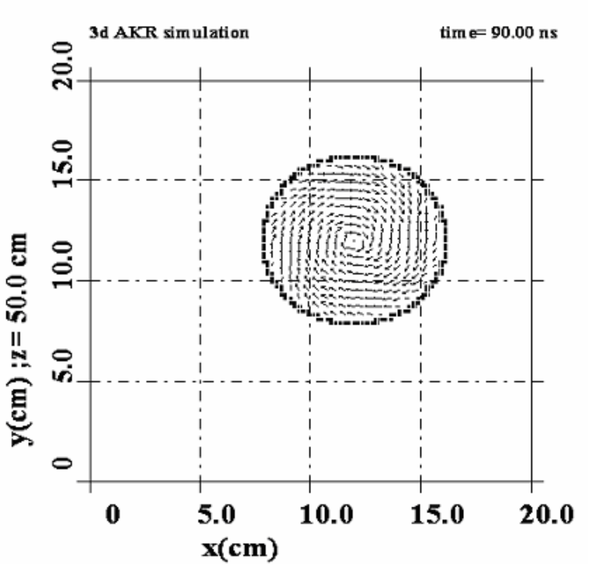

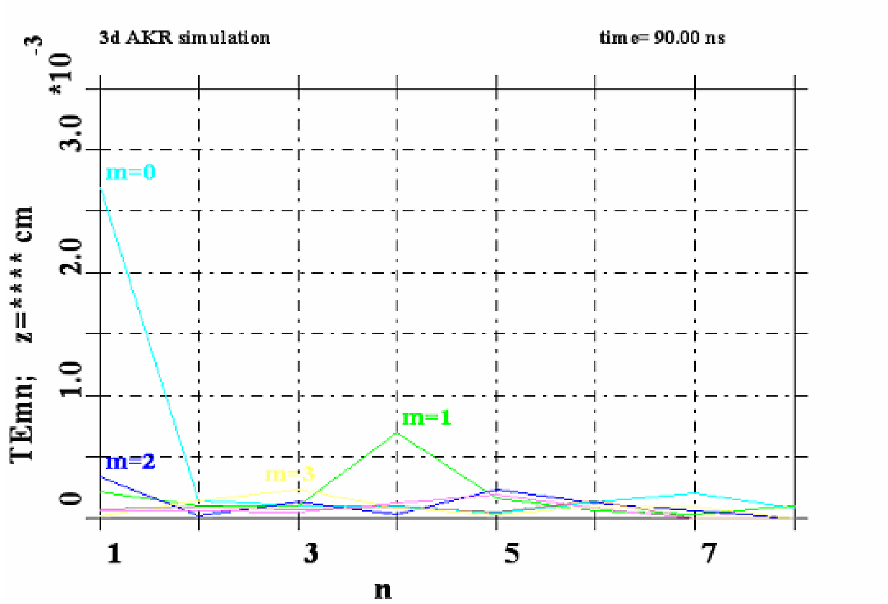

Microwave spectral measurements - 4.42GHz

- 12GHz Real-time oscilloscope
- AC waveform captured
- Fourier transform gives frequency

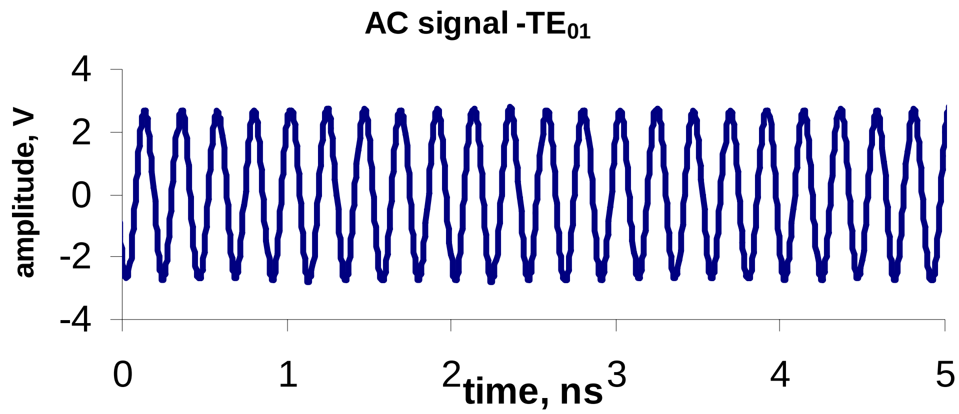

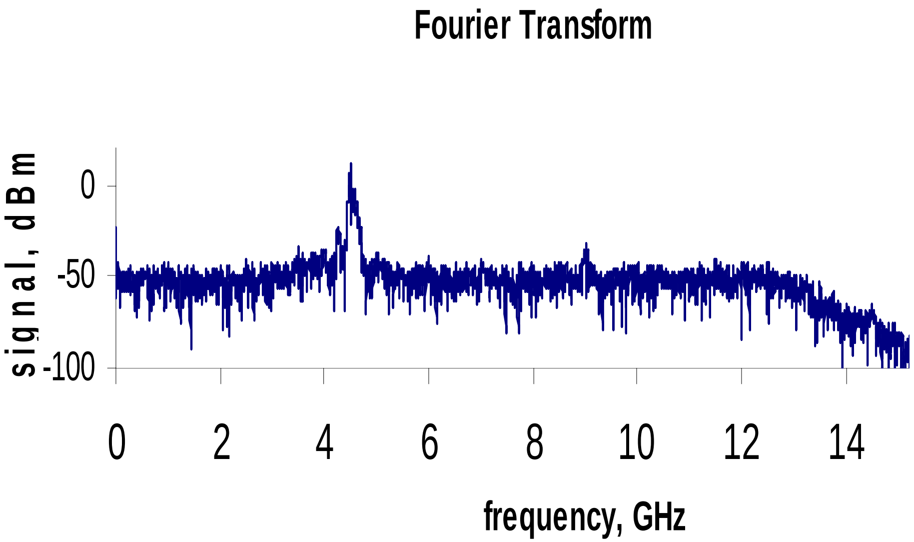

- Spectral peak at ~4.42GHz
- Close to cut-off for TE_{01}
- Second harmonic at ~8.84GHz

Microwave amplitude and polarisation measurements at 4.42GHz

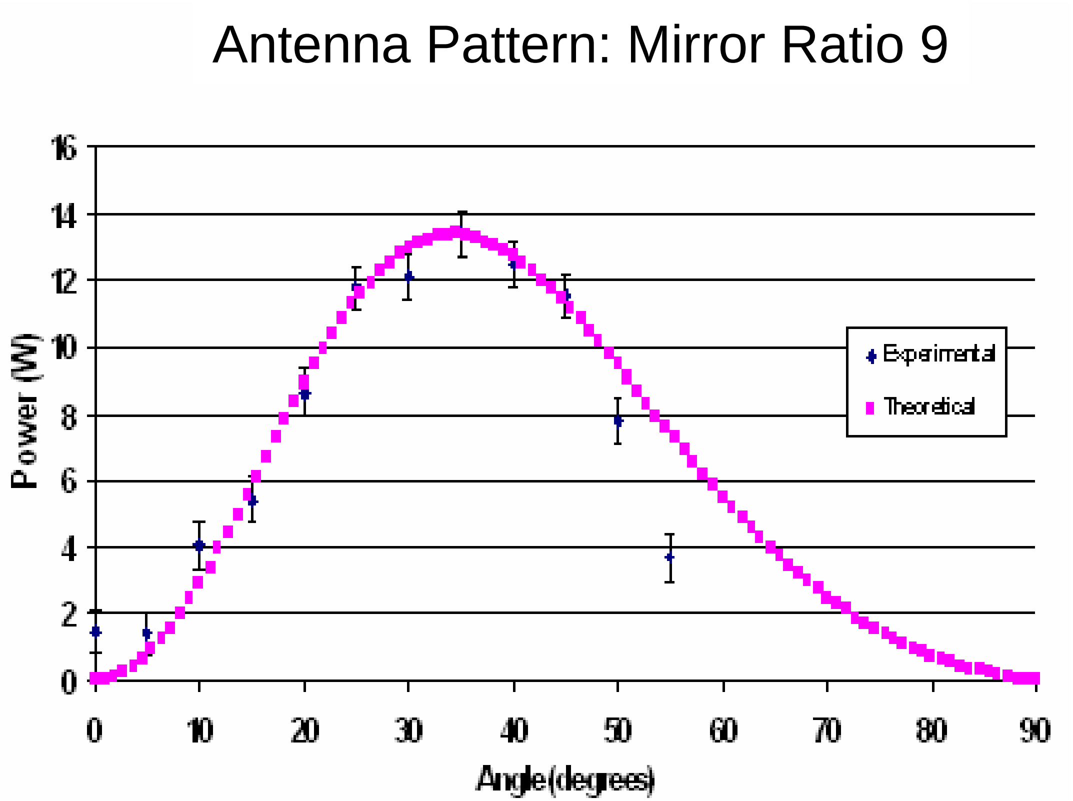

- Integrated antenna pattern:
- Radial polarisation gave no output
- Azimuthal polarisation:

  Cathode B=0.011T ~ 19 kW

  Cathode B=0.02T ~ 35 kW
- Results consistent with 1D number density measurements
- Max efficiencies of ~2% for mirror ratio of 17, despite lower power
- Highest η at cyclotron detuning 2.4%

Comparison of numerical and experimental results

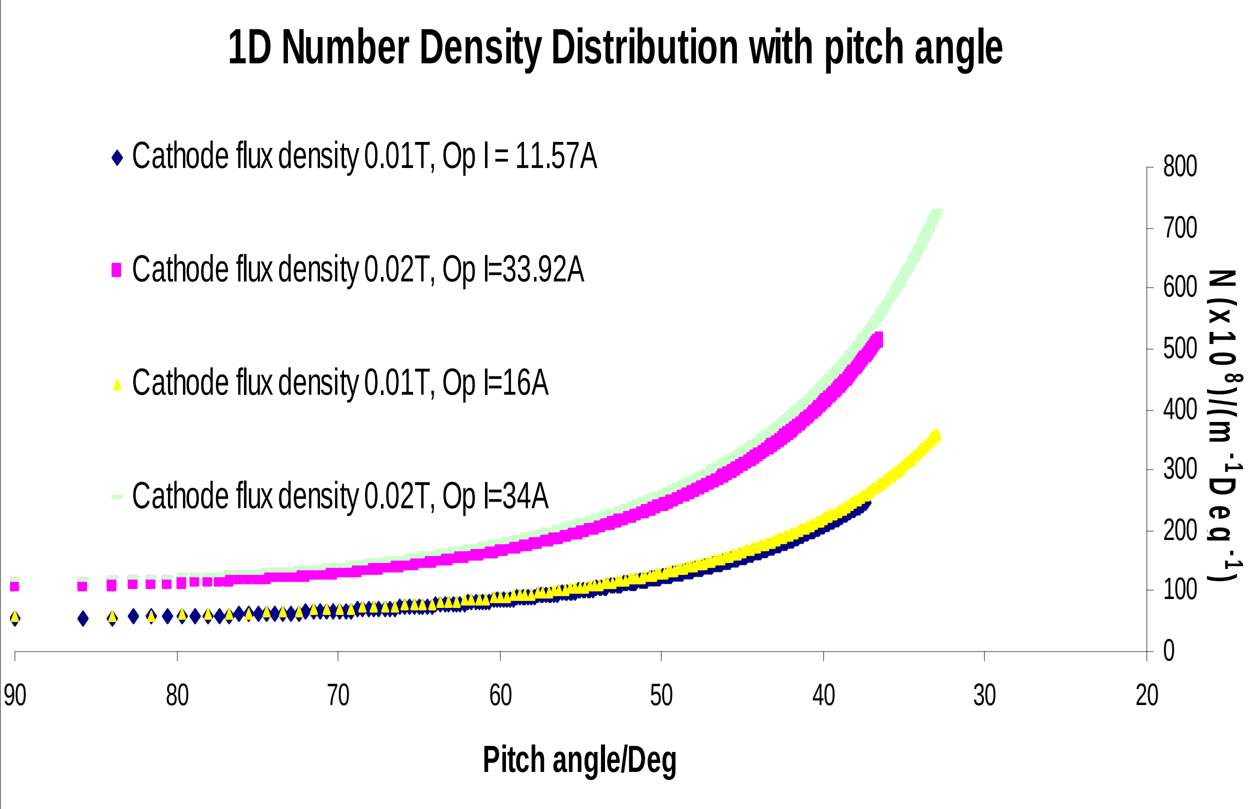

For cathode flux density 0.01T

Exp	Num
I_{in}=121A	I_{in}=18A
I_{out}=11.57A	I_{out}=16A
P_{out}=19kW	P_{out}=20kW

For cathode flux density 0.02T

Exp	Num
I_{in}=208A	I_{in}=35A
I_{out}=33.92A	I_{out}=34A
P_{out}=35kW	P_{out}=50kW

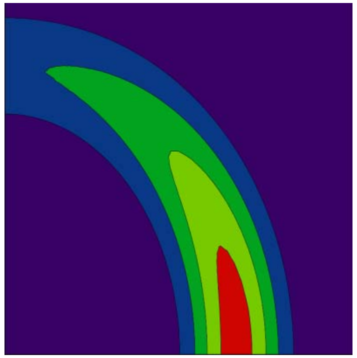

- Pitch angle is arctan($v_\perp / v_z$)

11.7GHz 2D Numerical Results

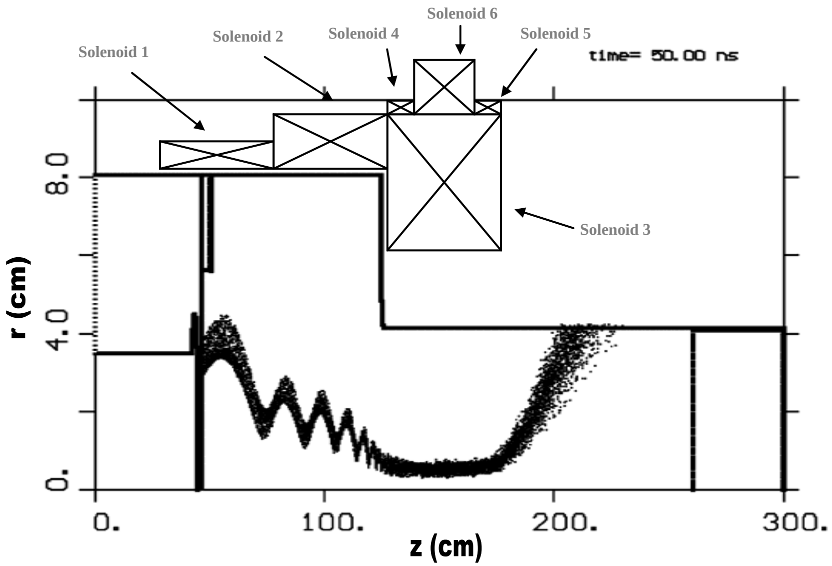

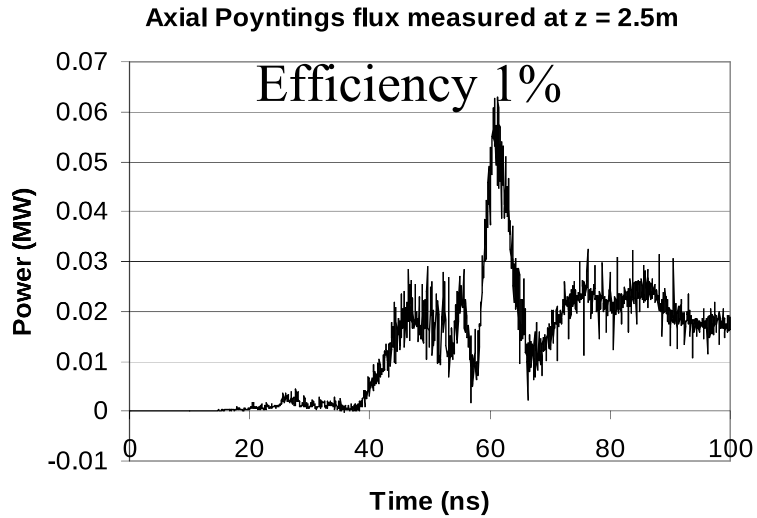

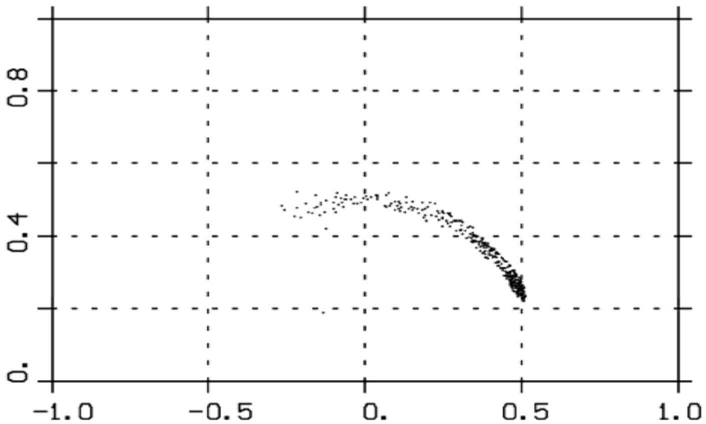

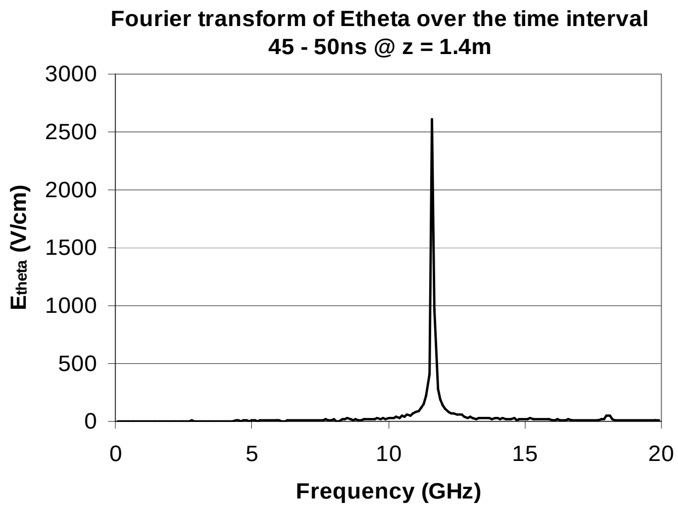

11.7GHz 3D Numerical Simulations

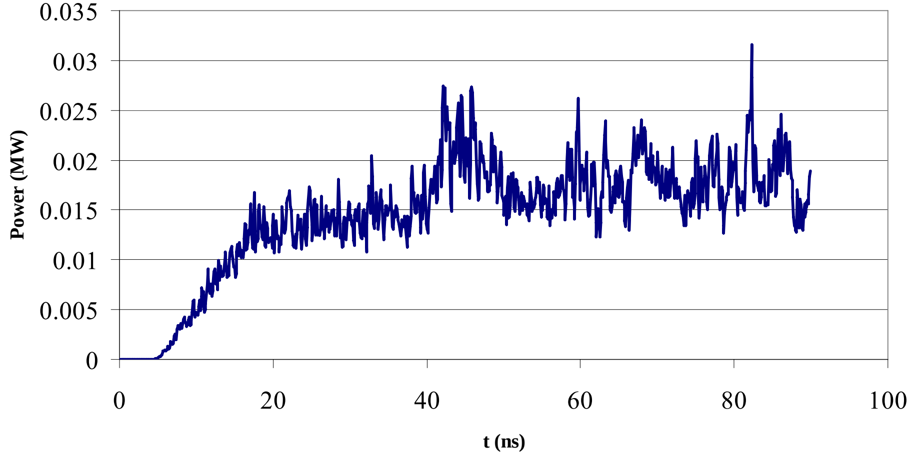

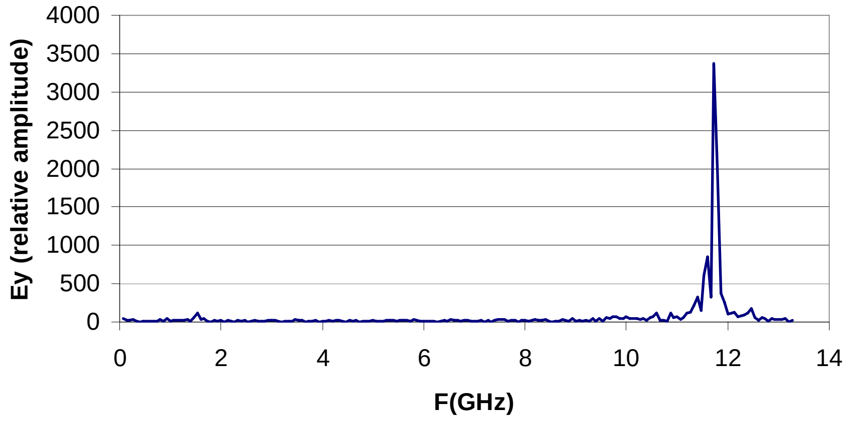

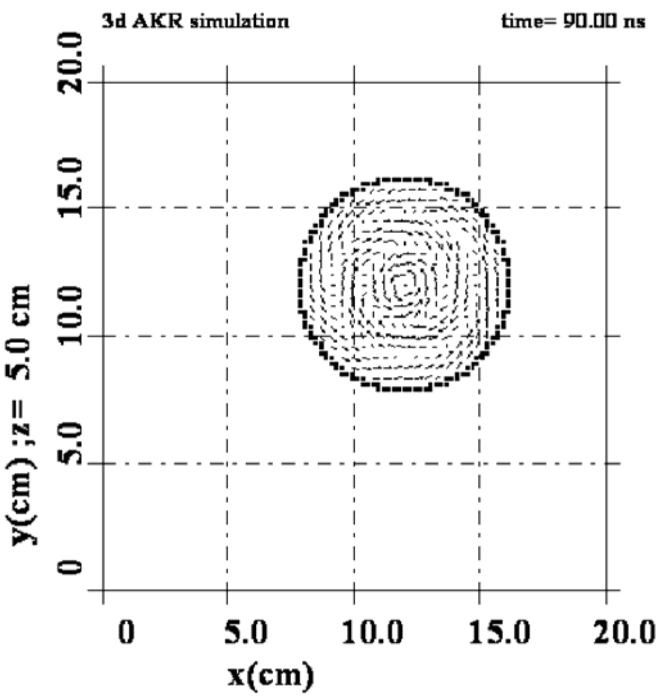

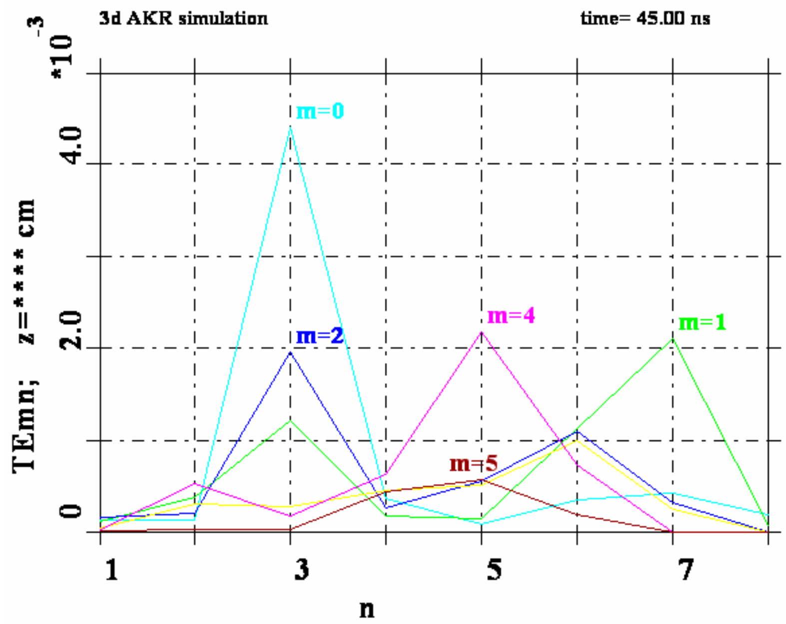

Microwave Spectral Measurements- 11.7GHz

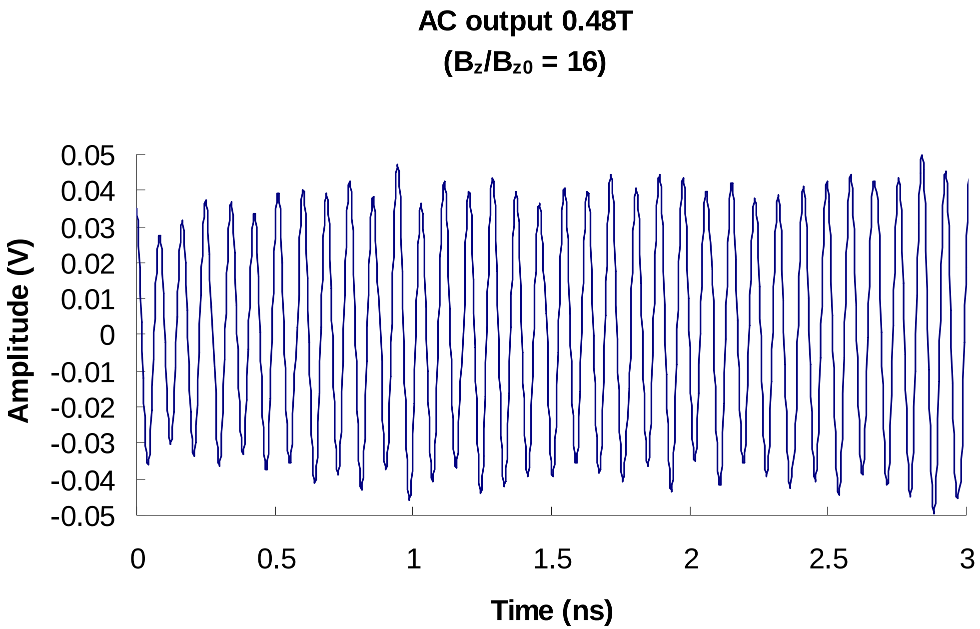

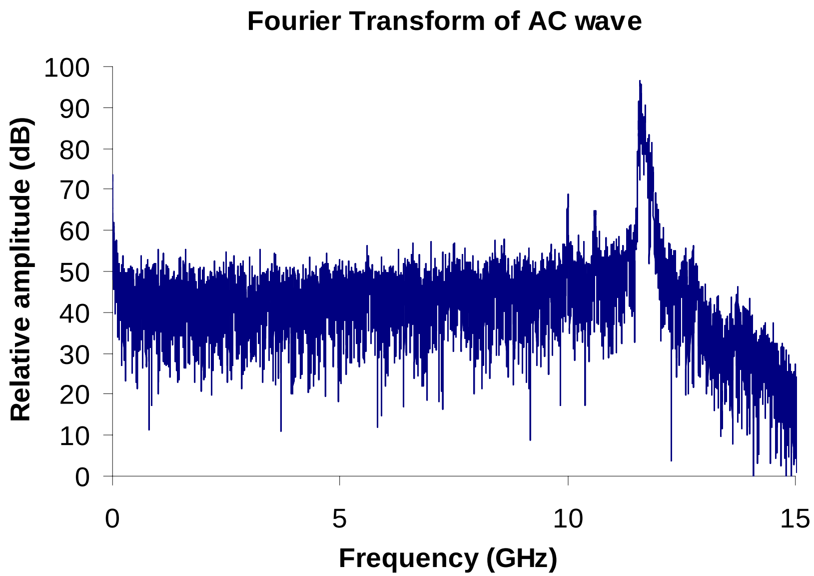

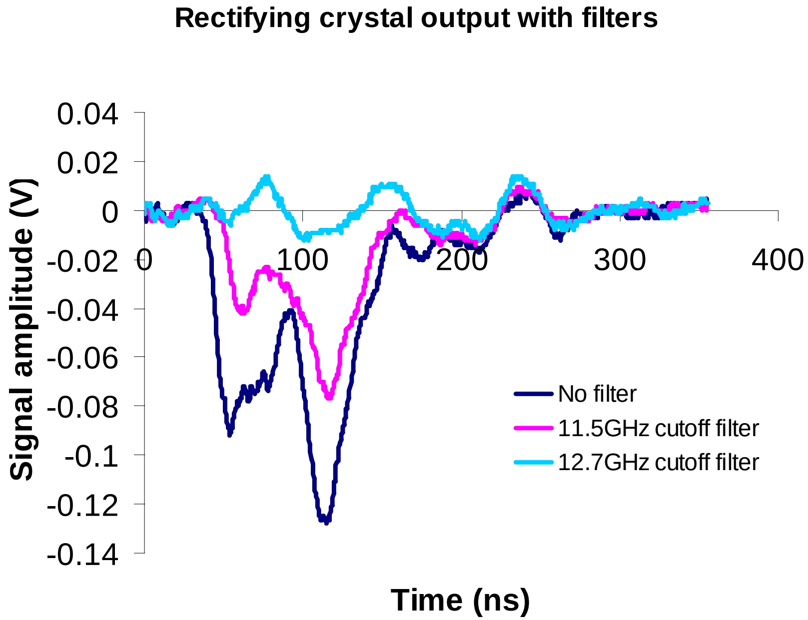

- Spectral peak at 11.7GHz
- Evidence of backward wave Doppler downshift component
- Close to cut-off for TE_{03}
- Close to CRO Bandwidth
- Check with waveguide filters

Microwave amplitude and polarisation measurements at 11.7GHz

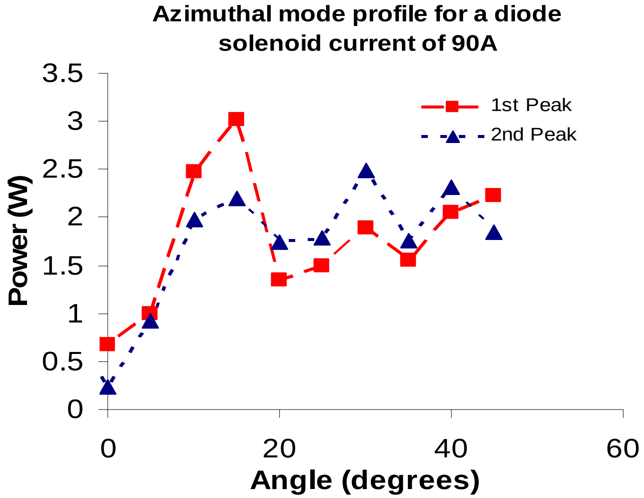

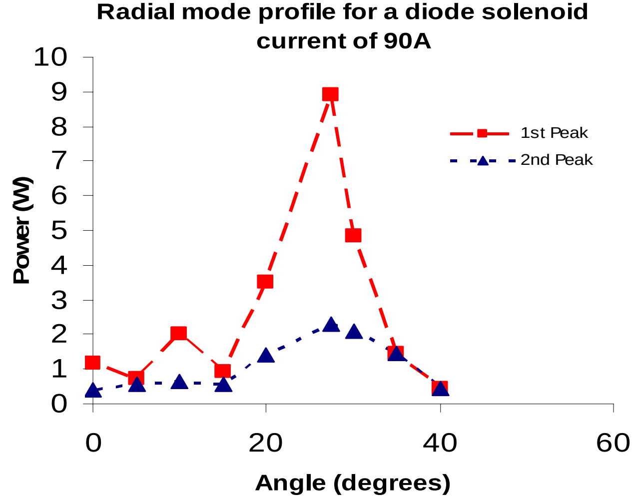

- Antenna Pattern indicated complex mode mixture
- Dominant mode changed with time
  -mode competition and hopping
- Radiation in both polarisations
- TE_{03} and TE_{23} modes present
- Integration of antenna pattern
- Max efficiencies of ~1% with peak output power ~20kW

Conclusion

- Succeeded in forming electron beam with Horseshoe velocity distribution
  - Number density mapped as a function of pitch angle
- Numerical simulations predict instabilities with efficiencies ~1-2%
- Microwave measurements confirmed instability of distribution to cyclotron emissions
  - Radiation frequency slightly > relativistic cyclotron frequency
- The antenna pattern measurements illustrated near cut-off TE modes as numerically predicted
- Experimental efficiencies comparable with the numerical predictions
- Wave polarisation, propagation similar to X mode
- Generation efficiencies compare well with some auroral estimates

Future work

- Investigate Doppler shifted regimes of resonance
  - Measure the resilience of the instability to parallel propagation
  - Build convective experiment to measure spatial growth rate

- Bridge gap to unbounded geometry
  - Numerical simulations underway to study cyclotron instabilities in the absence of ‘hard’ radiation boundaries

- Investigate influence of background plasma
  - Numerical studies underway of magnetised-plasma loaded waveguides
  - Experimental modification to include a plasma background- possibly a quasi-Penning trap

Acknowledgements

This work was supported by the EPSRC and the STFC centre for fundamental physics. Mr I. S. Dinwoodie and Mr D. Barclay are thanked for building the apparatus and Prof. V.L. Tarakanov for advice on the numerical codes.